Korhonen, Oona; Sawada, Daisuke; Budtova, Tatiana

All-cellulose composites via short-fiber dispersion approach using NaOH–water solvent

Published in:
Cellulose

DOI:
10.1007/s10570-019-02422-z

Published: 30/05/2019

Document Version
Peer-reviewed accepted author manuscript, also known as Final accepted manuscript or Post-print

Submitted to Cellulose 21 November 2018
Revised 29th March 2019

All-cellulose composites via short-fiber dispersion approach using NaOH-water solvent

Oona Korhonen[1], Daisuke Sawada[1], Tatiana Budtova[1,2]*

[1] Aalto University, School of Chemical Engineering, Department of Bioproducts and Biosystems, P.O. Box 16300, 00076 Aalto, Finland

[2] MINES ParisTech, PSL Research University, CEMEF – Center for materials forming, UMR CNRS 7635, CS 10207, 06904 Sophia Antipolis, France

Corresponding author: Tatiana Budtova

Email: Tatiana.Budtova@aalto.fi; Tatiana.Budtova@mines-paristech.fr

Phone: +33 4 93 95 74 70

Acknowledgements

The financial support from Business Finland, Stora Enso Oyj and UPM-Kymmene Oyj is gratefully acknowledged. Authors also want to thank to Separation Research Oy Ab and Fibertus Oy for collaboration; Herbert Sixta, Mark Hughes and Michael Hummel (Aalto University) for fruitful discussions, Suzanne Jacomet (CEMEF, MINES ParisTech) for assistance with SEM, Rita Hatakka (Aalto University) for help with pulp composition determinations as well as Hannu Revitzer (Aalto University) for elemental analysis. We thank Dr. Isabelle Morfin (ESRF) for assistance at the D2AM beam line, and ESRF (Grenoble, France) for the provision of beam time. At the D2AM beam line, the WAXS Open for SAXS detector (WOS) was funded by the French National Research Agency (ANR) under the "Investissements d'avenir" program, grant number: ANR-11-EQPX-0010.

Abstract

All-cellulose composites were prepared by dispersing short softwood kraft fibers in dissolving pulp-8 wt% NaOH-water. The degree of polymerization (DP) of the dissolving pulp used for the matrix and the concentration of reinforcing fibers were varied. Morphology, density, crystallinity, cellulose I content and mechanical properties of the composites were investigated. A special attention was paid on the presence of non-dissolved fibers originating from incomplete dissolution of pulp in 8 wt% NaOH-water thus decreasing the actual concentration of dissolved cellulose in matrix solution. This "lack of matter" induced the formation of pores, which strongly influenced the morphology of composites. Density was shown to be the main parameter contributing to the mechanical properties of the prepared all-cellulose composites. The results demonstrate the complexity of the system and the need in taking into account the dissolution power of the solvent.

Key words: all-cellulose composites, NaOH, dissolution, density, mechanical properties

Introduction

Modern society is trying to replace fossil-based materials by those made from renewable resources. Cellulose is a widely available natural polymer, and cellulosic fibers are seen as an attractive alternative to glass fibers for reinforcing polymers. However, chemical incompatibility between a traditional polyolefin matrix and cellulose fibers leads either to the insufficient composite mechanical properties or to the need of compatibilizers. One solution to overcome this problem is the so-called single-polymer composite approach, where both matrix and reinforcement originate from the same matter (Capiati and Porter 1975; Ward and Hine 1997).

All-cellulose composites are single-polymer composites based on cellulose (Nishino et al. 2004; Huber et al. 2012a). Since cellulose does not melt, all-cellulose composites are produced via dissolution-coagulation-drying route. All-cellulose composites can be divided into two main categories, depending on the type of continuous phase. In the first one, fibers (or fabric) make a continuous phase in which cellulose solvent is added; due to the partial dissolution of fibers' surfaces they are "glued" together (Soykeabkaew et al. 2008; Huber et al. 2013; Haverhals et al. 2012; Dormanns et al. 2016). In a similar way, all-cellulose composites were produced via impregnation of isotropic pulp sheets (Gindl et al. 2006; Piltonen et al. 2016; Hildebrandt et al. 2017; Sirviö et al. 2017), filterpaper (Nishino and Arimoto 2007; Duchemin et al. 2016) or anisotropic paper (Kröling et al. 2018) with a solvent, which results to fiber surface dissolution. Such "long-fiber" approach in all-cellulose composite production has been studied more systematically. In the second category, the continuous phase is represented by cellulose solution, in which short cellulose fibers are dispersed. This approach got much less attention compared to "long-fiber" counterpart, though short fibers provide a reinforcing material with low cost and suitability for composite bulk production. In the present work, only "short-fiber" composites will be considered.

The “short-fiber” all-cellulose composites can be produced via cellulose incomplete dissolution (many studies use microcrystalline cellulose) (Gindl and Keckes 2005; Duchemin et al. 2009; Abbot and Bismarck 2010) or through fiber dispersion in cellulose solution (Ouajai and Shanks 2009; Yang et al. 2010; Nadhan et al. 2012; Labidi et al. 2019). The latter mimics the production of conventional short-fiber polymer composites. This method should allow a rather easy control of cellulose concentration in the continuous phase and fiber concentration in the matrix. Dispersed fibers can also be nanofibrils (Yang et al. 2016) or cellulose nanocrystals (Pullawan et al. 2012; Pullawan et al. 2014; Lourdin et al. 2016), but these special cases will not be considered since they are out of the scope of this work.

Until now, three solvents have been used to prepare all-cellulose composites with “short-fiber” approach. The most studied is lithium chloride/dimethylacetamide (LiCl/DMAc) (Gindl and Keckes 2005; Duchemin et al. 2009; Abbot and Bismarck 2010) along with NaOH-water without additives (Labidi et al. 2019) or with urea (Yang et al. 2010; Nadhan et al. 2012), and N-methyl-morpholine-N oxide monohydrate (NMMO) (Ouajai and Shanks 2009). Aside the solvent type and the grade of cellulose used for the matrix and as reinforcing fibers, other numerous processing parameters can be varied. These are the concentration of cellulose in the matrix, concentration of reinforcing fibers, fiber size and aspect ratio, the conditions of partial dissolution or mixing (time, temperature) as well as coagulation and drying conditions (type of non-solvent, utilization of compression, drying method, etc.). Due to very different processing conditions, the reported mechanical properties vary by orders of magnitude and the influence of the reinforcing fiber concentration is not well understood. Thus, the first question to answer is as follows: does the increase of the concentration of reinforcing fibers ultimately leads to the improvement in modulus and strength, as in the case of thermoplastic composites?

6-9 wt% NaOH-water is proven to dissolve cellulose at subzero temperatures (Davidson 1934); it represents a low cost “green” solvent with existing recycling methods used in pulping industry.

However, the dissolution capacity of this solvent is limited by cellulose degree of polymerization (DP) and concentration (Kamide et al. 1992; Egal et al. 2007), and solutions are gelling with time and temperature increase (Roy et al. 2003). These drawbacks are among the main reasons why this solvent is not used by industry for making cellulose fibers and films. The second question to answer is how and if these solvent limitations influence "short-fiber" all-cellulose composite processing and properties?

The goal of this work is to answer the two questions mentioned above by performing a systematic study of the morphology and properties of short-fiber reinforced all-cellulose composites. We used 8 wt% NaOH-water as cellulose solvent and varied the DP of initial matrix pulp and reinforcement content by dispersing softwood kraft fibers into dissolving pulp-NaOH-water solution. The novelty of our approach consists in unravelling the influence of solvent power on the morphology and properties of all-cellulose composites. We demonstrate that "good adhesion" principle, which is the main argument of all-polymer composites, may not always be a sufficient condition in case of cellulose. Density, morphology, cellulose I volume fraction, crystallinity and tensile properties of the produced all-cellulose composites were determined, and the effect of the matrix pulp DP and reinforcement content on composites' properties was analyzed.

Experimental section

Materials

Birch dissolving pulp and softwood kraft fibers were kindly provided by Stora Enso Oyj. Dissolving pulp was used for the matrix and kraft fibers as short reinforcing fibers. The viscosity-based degree of polymerization (DP) of dissolving pulp and kraft fibers was 1100 and 2550, respectively (see details on DP determination in Methods). Three pulp DPs were used for the matrix: 1100 (the initial dissolving pulp), 650 and 330, the two latter obtained from the initial one by acid hydrolysis (see details on acid hydrolysis in Methods section).

All dissolving pulps had cellulose content of 92 wt%, hemicellulose content of 7 wt% and lignin content < 1 wt% (see details on pulp composition determination in Methods). Kraft fibers contained 80 wt% of cellulose, 19 wt% hemicellulose and < 1 wt% of lignin. All lignin contents were originating from acid-soluble lignin fraction, no Klason lignin was detected.

NaOH was purchased from VWR International as solid flakes and dissolved in deionized water to obtain 8 wt% NaOH-water solution. Lithium chloride (LiCl) was purchased from Merck and both dimethylacetamide (DMAc) and acetone were from VWR Chemicals BDH Prolabo.

The initial pulps were provided as air-dry sheets and the acid hydrolyzed pulps were air dried in room temperature (93-96 % dry matter content); all concentrations are given in wt%.

Methods

Pulp characterization and acid hydrolysis

Fiber length and width distributions of the pulps used for matrix and of kraft fibers was obtained with FiberLab™ (Metso Automatization), each type was analyzed in triplicate. The mean values are calculated as arithmetic averages provided by the device.

The carbohydrate and lignin contents in the pulps were determined according to the analytical method NREL/TP-510-42618. Monosaccharides were detected via high-performance anion exchange chromatography with pulse amperometric detection (HPAEC-PAD) in a Dionex ICS-3000 column and they were transferred to carbohydrates according to Janson (1970).

The DP of pulps was determined via intrinsic viscosity, based on cellulose dissolution in cupriethylenediamine (CED), according to the standard SCAN-CM 15:88. The DPs were calculated using the Mark-Houwink equation suggested by the norm.

The DP of the dissolving pulp was varied via acid hydrolysis with sulfuric acid; it was conducted at 3 % consistency for 60 minutes under overhead mixing at controlled temperature. In order to decrease the DP from 1100 to 650 and 330, the temperatures were set to 82 °C and 88 °C

and the acid concentrations were 0.1 M and 0.6 M, respectively. After acid hydrolysis, samples were washed with deionized water until neutral pH was reached. Subsequently, pulps were air dried overnight in a fume hood and disintegrated with a laboratory mill. The gravimetric yield was 98 ± 1 % for both pulps.

Acid hydrolysis decreased the average molar mass of the pulps, as expected, and changed the polydispersity from 4.7 to 3.3 and 2.3 for DP 1100, 650 and 330, respectively (see Figure S1 in Supplementary Data). Molecular weight distributions were determined via gel permeation chromatography (GPC) consisting of pre-column (PLgel Mixed-A, 7.5, 50 mm), four analytical columns (PLgel Mixed-A, 7.5, 300 mm) and a RI-detector (Shodex RI-101). Samples were dissolved in LiCl/DMAc after activation in water, acetone and DMAc; the detailed procedure is explained by Michud et at. (2015). Acid hydrolysis had no effect on the composition of the pulp within experimental errors.

Determination of cellulose solid (non-dissolved) fraction after dissolution in 8 wt% NaOH-water

The dissolution of cellulose in 8 wt% NaOH-water is strongly depending on cellulose DP and concentration (Budtova and Navard 2016), and it is known that the dissolution can be incomplete for high DP cellulose (Kamide et al. 1992). Thus, we determined the remaining solid (non-dissolved) fraction in the 5 wt% pulp-8 wt% NaOH-water solution for each dissolving pulp used to make composite matrix:

$$Solid\ fraction, \% = \frac{m(residue)}{m(dissolving\ pulp)} \times 100\% \quad (1)$$

where *m(dissolving pulp)* is the oven-dried weight of the pulp placed in the solvent and *m(residue)* is oven-dried weight of the non-dissolved fraction (see the details below). *Solid fraction* is 0 % when the dissolution is complete (no residues) and is 100 % in the case of no dissolution. For simplicity, we use here the term “solution” for all cases. As it will be shown later, for the pulps of

170 DP 650 and 1100 non-dissolved fibers were present, and thus these systems are fiber suspensions in
171 cellulose-NaOH solution. The presence of non-dissolved fibers was confirmed via optical
172 microscope (LEICA DM750 with a camera LEICA ICC550 HD).

173 The weight of *m(residue)* was determined as follows. Cellulose solutions were prepared by
174 dissolving 5 wt% of pulp in 8 wt% NaOH-water following the same procedure used for composite
175 preparation described in the next section. Solutions were centrifuged for 15 minutes under 11 000
176 rpm (Eppendorf Centrifuge 5804R) to separate the non-dissolved solid fraction from the dissolved
177 phase. The solid residue was washed twice with 8 wt% NaOH-water to remove the remaining
178 cellulose solution attached to non-dissolved fibers. Subsequently, the solid fraction was washed
179 with deionized water until neutral pH, and filtered through paper filter (Whatman, 589[3], ashless).
180 The residue was dried at 105 °C overnight and its weight *m(residue)* was measured. The solution
181 with the pulp of DP 650 had high viscosity and to separate the solid fraction it had to be diluted
182 with 8 wt% NaOH-water (1:1) prior to centrifuging; other solutions were not diluted. The
183 measurements for all pulps were performed in duplicate.

184 The size distributions (length, width and aspect ratio) of particles in the non-dissolved fraction
185 was determined by measuring their sizes using optical microscope. A sample of pulp solutions of
186 DP 650 and 1100 were diluted (1:30) with 8 wt% NaOH-water in order to better visualize the
187 individual particles. Microscopic images were taken by LEICA DM 750 (camera LEICA ICC550
188 HD) and particles' dimensions were measured with LAS EZ software; at least 80 individual
189 particles were analyzed and mean fiber sizes were calculated as arithmetic averages.

190

191 *All-cellulose composite preparation*

192 The pulps were provided as air-dry sheets and they were disintegrated by a laboratory mill. All-
193 cellulose composites were produced via dissolution-mixing-coagulation-compression-drying route
194 (Figure 1). First, 5 wt% solutions of dissolving pulp were prepared in pre-cooled 8 wt% NaOH-

water using overhead mixer (Heidolph, 300 rpm) at -7 °C for 2 hours. Kraft fibers were wetted with 8 wt% NaOH-water (dry pulp: NaOH solution = 1:4) in order to ease their mixing with pulp solution. The solution was removed from the cooling bath and fibers were added while the solution remained cold (within 15 min, before gelation starts); in these conditions kraft fibers did not dissolve. The mixture was placed in a Petri dish and gelled at 50 °C for one hour. NaOH was then removed by washing in water (diluting by approximately 1:100) at 50 °C for two days by exchanging water twice a day. Washed samples contained 0.004-0.02% of sodium, which indicates that washing procedure was successful. Sodium content was determined via elemental analysis, with air-acetylene flame in AAS-device (Varian AA240) after dissolving the sample into 65 % nitric acid in microwave oven (Milestone Ethos) for one hour at 200°C.

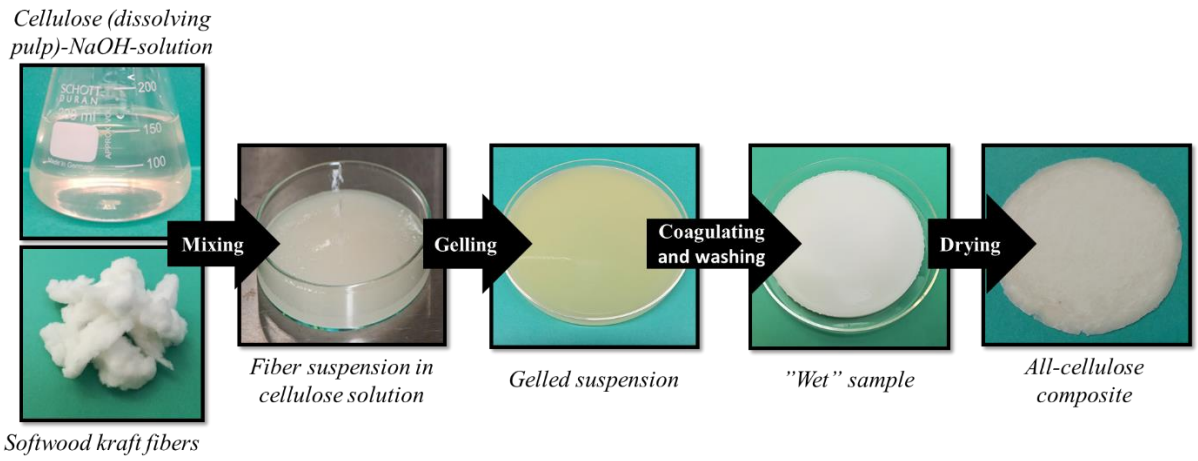

Fig. 1

Schematic presentation of the preparation of all-cellulose composites via short-fiber approach, together with the images of materials at each step

Washed samples (coagulated cellulose with water in the pores) were dried in two steps. First, most of the water was removed by compressing the composite at room temperature with 0.37 MPa pressure for 2 minutes (pneumatic sheet press L&W SE 040, Ab Lorentzen & Wettre). Second,

214 sample was hot-pressed at 100 °C for 2 hours with 3.9 MPa (Carver Laboratory Press). Dry samples
215 were non-transparent (Figure 1) and had thickness of 0.2-0.9 mm, which was increasing with the
216 reinforcement content. Samples were stored in sealed plastic bags at room temperature.
217
218 *Composite characterization*
219 All-cellulose composites were characterized regarding density, morphology, crystallinity,
220 cellulose I volume fraction and tensile properties. Bulk densities were determined by dividing the
221 mass of the oven-dry sample by its volume, the latter calculated from size measurements performed
222 with a digital caliper (Cocraft). The morphology of the samples was studied with scanning electron
223 microscopy (SEM, Phillips XL30). Samples were coated with 7 nm of platinum prior to
224 examination.
225 Synchrotron X-ray diffraction data were collected at beamline D2AM at ESRF (Grenoble,
226 France). The powder samples were tightly packed into a glass tube with an outer diameter of 3 mm
227 and wall thickness of 200 μm. The glass tubes were mounted on multi-position sample holder.
228 Wide-angle powder diffraction patterns were collected in the transmission mode on a flat 2D
229 detector (WOS). X-ray energy was set to 18 keV (λ = 0.688801 Å). Sample to detector distance was
230 calibrated using Cr_2O_3 powder.
231 The powder diffraction data were processed using pyFAI (Ashiotis et al. 2015), a python
232 library for azimuthal integration of diffraction data. The diffraction profiles were obtained from the
233 azimuthal averaging of raw 2D image correcting for the detector distortion. The diffraction profiles
234 were processed by normalizing to incident beam intensity, subtracting scattering contribution from
235 glass tube and subtracting inelastic scattering from the sample. The remaining elastic intensities
236 from the sample were processed by subtracting scattering contribution from amorphous domains.
237 The smoothing approach was employed to estimate the amorphous background (Brückner 2000;
238 Frost et al. 2009) applying Savitzky-Golay filter (Savitzky and Golay 1964) for 2θ from 3.5° to 20°.

239 Window size and polynomial order for the Savitzky-Golay filter were set to 51 and 1, respectively.
240 This method intends to smooth out only the peak characteristics in the scattering profile. Iteration
241 for the background estimation was repeated until the iteration does not reduce the background area
242 significantly. In these experimental and smoothing conditions, the smoothing procedure was
243 terminated by 20 smoothing cycles.

244 Crystallinity index (*CRI*) of all-cellulose composites was calculated from the ratio between the
245 area of total intensity (S_{total}) and background intensity (S_{bkg}) in the range of 2θ from 4° to 12° as
246 follows (Thygesen et al. 2005):

247 $$CRI\ \% = \left(\frac{S_{total} - S_{bkg}}{S_{total}}\right) \times 100\% \quad (2)$$

248 In order to calculate the volume fraction of cellulose I ($R_{Cell\ I}$) in all-cellulose composites, the
249 diffraction profiles from kraft fibers and dissolved pulp of DP 330 were also obtained and used as
250 references of cellulose I and cellulose II, respectively. Based on these reference spectra, 1000
251 "theoretical" diffraction profiles (I_{calc}) were calculated for different proportions of cellulose I and
252 cellulose II in all-cellulose composites by varying cellulose I composition from 0 to 100 with a step
253 of 0.1 as follows:

254 $$I_{calc} = I_{ref\ I} R_{Cell\ I} + I_{ref\ II}(100 - R_{Cell\ I}) \quad (3)$$

255 where $I_{ref\ I}$ is the reference intensity profile of kraft fibers, $I_{ref\ II}$ is the reference intensity profile of
256 dissolved pulp of DP 330. Diffraction profile from experimental data was then subtracted from the
257 theoretical profiles (I_{calc}) and $R_{Cell\ I}$ was determined when the difference was at minimum.

258 The tensile properties were studied according to standard ISO 1924-2 with METS 400/M
259 tensile testing device, with a speed of 0.5 mm/min and 200N load cell. At least five specimens of
260 each formulation were tested; they were conditioned for 24 hours in a controlled environment of 50
261 % relative humidity and 25 °C and tensile experiments were conducted in the same conditions.

262

263 **Results and Discussion**

Analysis of pulp solutions

The state of 5 wt% pulp solutions in 8 wt% NaOH-water is illustrated by optical microscopy images, see examples in Figure 2. Increasing the DP leads to higher solid fraction in a solution, with extremely high amount of non-dissolved fibers for the case of DP 1100. Table 1 shows the measured solid (or non-dissolved) fraction for each pulp in 8 wt% NaOH-water, and the actual concentration of dissolved cellulose, C (in wt%), calculated as follows:

$$C, \% = (1 - Solid\ fraction) \times C_0 \quad (4)$$

where C_0 is total oven-dry pulp concentration in 8 wt% NaOH-water, here 5 wt%.

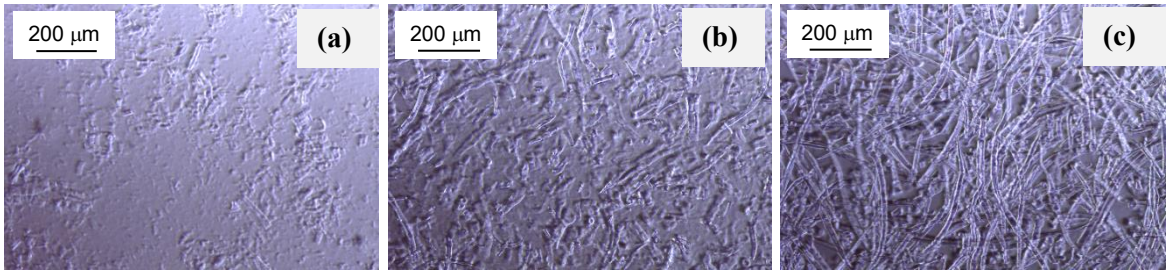

Fig. 2

Optical microscopy images of 5 wt% pulp-8 wt% NaOH-water solutions from pulps of (a) DP 330, (b) 650 and (c) 1100

Table 1. Non-dissolved solid fractions in 5 wt% solutions (Eq. 1), actual cellulose concentration in solution (Eq. 4), reinforcing fibers' concentrations (Eqs. 5-7).

	Matrix pulp DP 330				Matrix pulp DP 650				Matrix pulp DP 1100			
Solid fraction, wt%	4				34				77			
Dissolved cellulose concentration, wt %	4.8				3.3				1.2			
Added fibers (wet), wt %	2.9	3.7	6.4	6.9	0.9	2.4	4.0	6.6	0	3.9	6.6	7.4
Total reinforcement (wet), wt%	3.2	4.0	7.1	7.6	1.9	2.4	5.6	8.3	3.8	7.3	9.8	10.2
Reinforcement (dry), wt%	40	53	68	75	44	58	67	78	77	89	92	94

The fraction of solid (non-dissolved) cellulose varies from 4 % to almost 80 % with the increase of pulp DP, which is in accordance with the values reported by others (Kamide et al. 1992). This is a very important result for two reasons. First, it means that the fraction of the total reinforcement in all-cellulose composites will originate not only from the added reinforcing fibers (kraft fibers), but also from the non-dissolved fibers in the matrix. Second, the actual concentration of cellulose in solution, and thus in composite matrix, is lower than the planned 5 wt% as not all cellulose is dissolved. As it will be shown later, the insufficient amount of dissolved cellulose in the matrix results in decreased the mechanical properties of composites. When the DP of the dissolving pulp is 330, 4.8 wt% of cellulose was dissolved instead of initially targeted 5 wt%. However, in the case of matrix with DP 1100, only 1.2 wt% was dissolved. Similar results were reported for various pulps dissolved in NaOH-water: while almost 100% dissolution was reached for DP 300, the dissolution decreased to around 80% for DP 600 and was around 20-30% for DP 1000 (Kamide et al. 1992).

The dimensions of the fibers in the pulps before dissolution and in the solid (non-dissolved) fraction in matrix solutions are given in Table 2. After the dissolution, pulp of DP 330 had practically no solid content, as seen from Figure 2, but solutions of pulps of DP 650 and 1100 contained a large non-dissolved fraction. The aspect ratio of fibers before the dissolution was 18, 22 and 23 for pulps with DP 330, 650 and 1100, respectively. After the dissolution, the aspect ratio of solid fraction of DP 650 is around 4, and of DP 1100 is around 19. Indeed, the visual appearance of the solid fraction of DP 650 is a sort of “particles” while it is “fibers” for non-dissolved DP 1100 (see optical micrographs of the representative examples of non-dissolved fractions in Figure 3). Ballooning can be seen on fibers of non-dissolved fraction of DP 1100. Size distributions of the length, width and aspect ratio in the non-dissolved fraction as well as the fiber length and width distributions of all initial pulps are shown in Figure S2 of the Supplementary Data.

Table 2. Average values of length, width and aspect ratio of fibers in the pulps of DP 650 and 1100 before the dissolution and in the solid (non-dissolved) fraction. Standard deviations are in brackets

Pulp DP	Length, μm		Width, μm		Aspect ratio	
	initial	in non-dissolved fraction	initial	in non-dissolved fraction	initial	in non-dissolved fraction
650	323 (6)	185 (105)	15 (0.1)	52 (15)	22 (0.5)	4 (4)
1100	350 (<1)	416 (189)	15 (0.2)	24 (10)	23 (0.2)	19 (9)

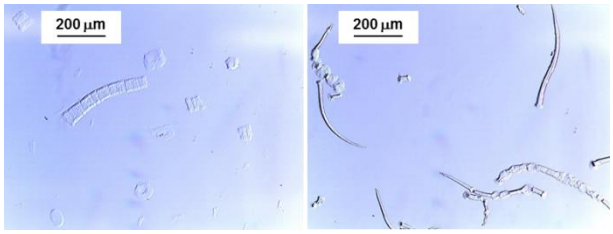

Fig.3

Optical microscopy images of the examples of solid (non-dissolved) fractions in solutions of pulps of DP 650 (a) and 1100 (b)

Concentration of reinforcing fibers in all-cellulose composites

During the preparation of all-cellulose composites, the concentration of cellulosic matter changes from the mixing (wet) to the final (dry) state. Several reinforcement concentrations should thus be considered (see equations 6 - 8), and fibers from the solid (non-dissolved) fraction of matrix solution must also be taken into account in the calculation of the concentration of reinforcing fibers.

The first reinforcement concentration, *Added fibers*, is the amount of kraft fibers added into dissolving pulp-8 wt% NaOH-water solution, and is thus noted “wet” (Equation 5). However, the total reinforcement content is increased when taking into account the non-dissolved fibers from the

matrix solution: it is given by *Total reinforcement (wet)*, as shown by Equation 6. Finally, the most important reinforcement concentration in all-cellulose composite is the reinforcement in the dry state, *Reinforcement (dry),* and it is described with equation 7.

$$Added\ fibers\ \%\ (wet)\ =\ \frac{m(kraft)}{m(solvent)+m(dissolving\ \ pulp)+m(kraft)} \times 100\% \qquad (5)$$

$$Total\ reinforcement\ \%\ (wet) = \frac{m(kraft)+m(solid\ fraction)}{m(solvent)+m(dissolving\ pulp)+m(kraft)} \times 100\ \% \qquad (6)$$

$$Reinforcement\ \%\ (dry\ )\ \ =\ \ \frac{m(kraft)+m(solid\ fraction)}{m(dissolving\ pulp)+m(kraft)} \times 100\ \% \qquad (7)$$

where *m(kraft)* is the oven dry weigth of added kraft fibers and *m(solvent)* is the weight of 8 wt% NaOH-water.

Table 1 gives all reinforcement concentrations, in dry and wet states, for all composites produced with pulps of different DPs. The reinforcement concentration obviously changes from the wet to dry state. The fraction of the reinforcement originating from the matrix itself (pulps with DP 650 and 1100) strongly influences the actual reinforcement content in the composites. For example, with ~ 4 wt% of added kraft fibers in solution, the composite based on matrix with DP 330 has 53 % of total reinforcement while it increases to 89 % for the matrix with DP 1100.

Morphology and properties of all-cellulose composites

The density of all-cellulose composites as a function of reinforcement content of dry samples is shown in Figure 4; density decreases from 1.16 to 0.81 g/cm^3 with increasing reinforcement content, which indicates increasing porosity from around 20% to around 45%, respectively. Porosity can be roughly estimated from the ratio of composite bulk to skeletal density, with the latter taken as 1.5 g/cm^3. Porous composites with even lower densities, around 0.5 – 1.0 g/cm^3, were reported for all-cellulose composites made from alfa fibers (Labidi et al. 2019) and by impregnating pulp sheets with NaOH-urea-water (Piltonen et al. 2016; Hildebrandt et al. 2017). The reinforcement content

349 plays the major role in the density of composites, and the DP of dissolved pulp has a minor effect
350 (Figure 4). Decreasing density of composites with high amount of reinforcing fibers indicates the
351 presence of voids. This is important to keep in mind when analyzing the mechanical properties of
352 composites.

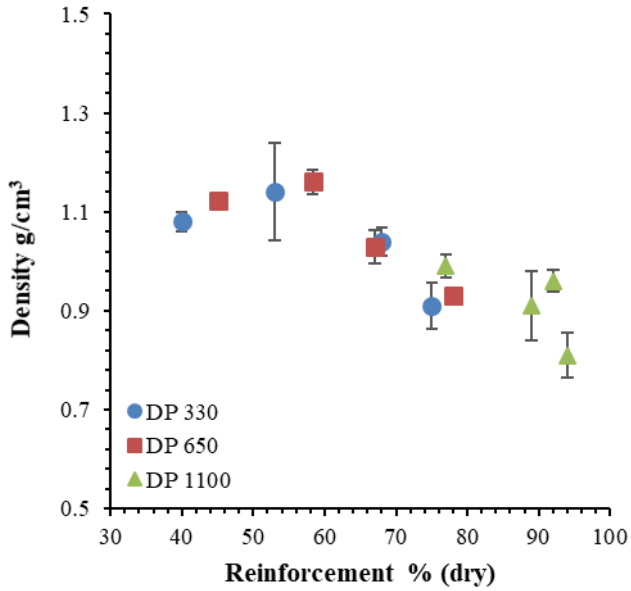

353

354 **Fig.4**

355 Density of all-cellulose composites as a function of reinforcement content expressed as dry
356 matter

357

358 The examples of surface morphology of all-cellulose composites are shown in Figure 5. An
359 excellent adhesion between the reinforcing fibers and the matrix occurs for the case of the
360 dissolving pulp DP 330 (Figure 5a). The fibers are homogeneously distributed in the matrix to form
361 a network, which is "glued" by the matrix. However, when the reinforcement content is very high,
362 originating from non-dissolved fibers of the matrix itself (DP 1100), a large number of voids
363 appears (Figure 5b), which is reflected by low density. The reason is the poor dissolution of high
364 DP dissolving pulp. There is simply not enough matter to form a continuous matrix with such a
365 high reinforcing content of randomly oriented fibers (Table 1).

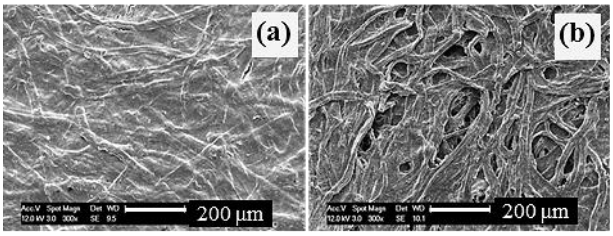

Fig. 5

SEM images of all-cellulose composites based on matrix with dissolving pulp (a) DP 330, 53% reinforcement (dry) and density 1.1 g/cm^3 and (b) DP 1100, 94% reinforcement (dry) and density 0.8 g/cm^3

The volume fraction of cellulose I ($R_{Cell\ I}$) in all-cellulose composites and their crystallinity were determined using XRD, as described in Methods section. The examples of the representative diffraction profiles together with data processing are shown in Supplementary Data, Figure S3. The X-ray diffraction intensity is proportional to the volume fraction of certain crystal phase in case of a "mixture" of polymorphs (Alexander and Klug 1948), and thus the diffracted intensity can be used to quantify the volume fraction of each crystalline phase in all-cellulose composites. $R_{Cell\ I}$ is plotted as a function of the total reinforcement % (dry) in the composites (Figure 6) with the lowest value corresponding to the case of dissolved pulp of DP 330 without any fibers added. It should be noted that the volume fraction of cellulose I is estimated solely from the crystalline phase, whereas total reinforcement is estimated gravimetrically from all components including non-crystalline fraction of cellulose fibrils; some small differences between the two values are thus presumed. As expected, the increase of the reinforcement content (i.e. non-dissolved and added kraft) resulted in the increase of cellulose I volume fraction.

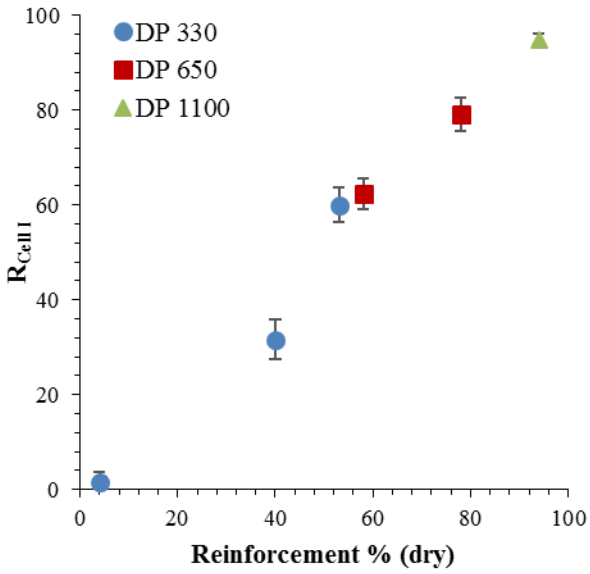

Fig. 6

Volume fraction of cellulose I in all-cellulose composites as a function of total reinforcement % (dry).

The crystallinity of composites varies between 36 and 50 % and practically does not depend on reinforcement concentration (see Supplementary Data, Figure S4). The reason is that kraft fibers have rather low crystallinity, around 42%, and the crystallinity of the separated solid (non-dissolved) fraction is around 33 – 36% for both DP.

A classical way to describe the mechanical properties of composites is to plot Young's modulus as a function of reinforcing fiber concentration. It is then expected that higher amount of reinforcing fibers would result in stronger composites. This turned out not to be true for all-cellulose composites prepared with pulps dissolved in 8 wt% NaOH-water. Young's modulus vs. reinforcement concentration is shown in Figure 7. Surprisingly from the first glance, Young's modulus decreases with increasing of reinforcing fiber content; the same was obtained for tensile strength (Figure S5, Supplementary Data). Crystallinity, being similar for all composites, cannot explain this phenomenon. No clear correlation between crystallinity and mechanical properties of all-cellulose composites is reported in literature. For example, when all-cellulose composites were

made by the impregnation of pulp sheets with NaOH-urea (Piltonen et al. 2016; Hildebrandt et al. 2017; Sirviö et al. 2017), the crystallinity was very high, around 80-90%, and it either did not vary (Sirviö et al. 2017) or slightly decreased (Piltonen et al. 2016) with the increase of the impregnation time (i.e. decrease of cellulose I fraction). The mechanical properties of these composites increased with the increase of impregnation time (Sirviö et al. 2017; Piltonen et al. 2016).

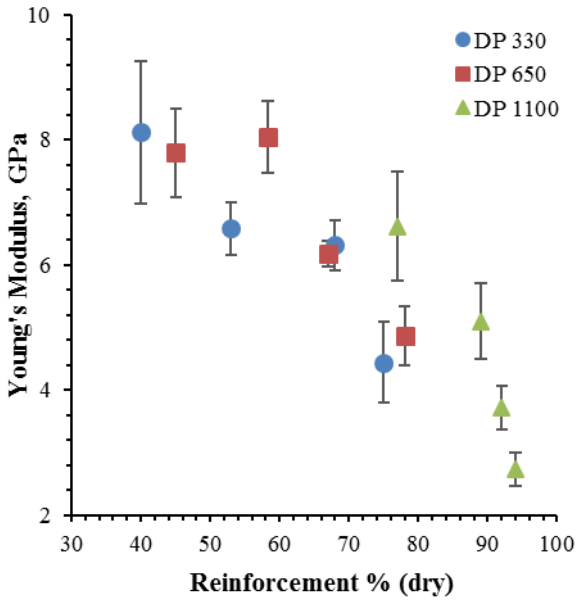

Fig. 7

Young's modulus of all-cellulose composites as a function of the reinforcement content in dry samples

The reason of the mechanical properties decrease with the increase of reinforcement content is the corresponding increase in porosity of the composites, which can be seen from decreasing density (Figure 4). Porosity is especially high for the case of high-DP pulps: the amount of matrix is insufficient for the high fiber content. It may also be possible that the compression of wet coagulated samples created structure defects leading to the appearance of voids. Composite density has thus to be taken into account when evaluating the mechanical properties of all-cellulose

composites. This is shown in Figures 8a and 8b for both Young's modulus and tensile strength, respectively. Higher composite density results in stronger composites, as expected. The elongation at break is low, around 1 %, and does not depend on reinforcing fiber concentration or matrix DP (see Supplementary data Figure S6).

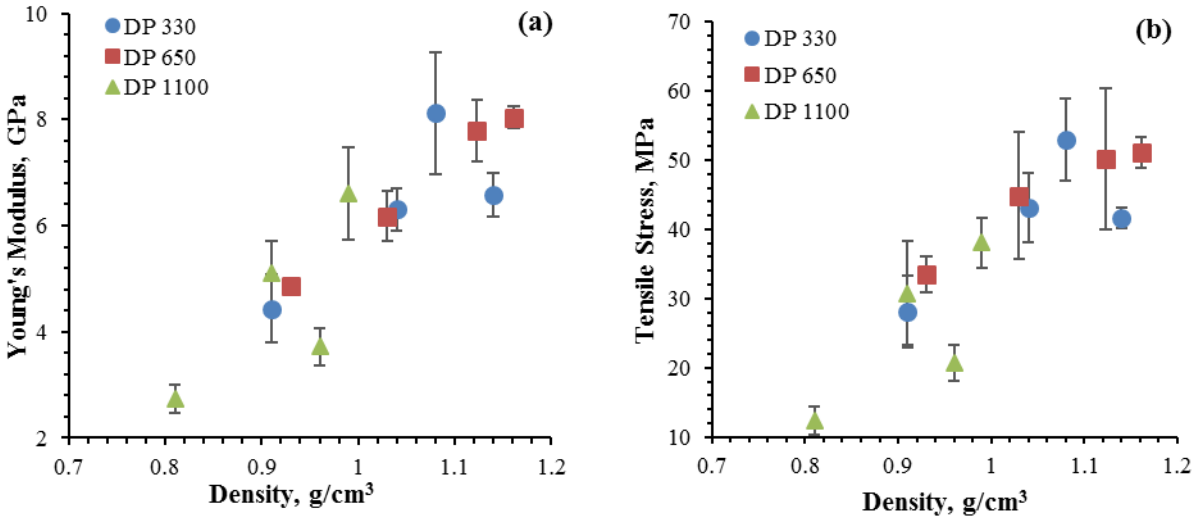

Fig. 8

(a) Young's modulus and (b) tensile strength vs. density of all-cellulose composites

Young's modulus varies from 2 to 8 GPa and tensile strength from 12 to 51 MPa for composites with densities from 0.81 to 1.16 g/cm^3, respectively. Similar results were obtained for natural fiber-polymer composites (Sobczak et al. 2012), in particular, for kraft fiber-polypropylene composites (Sobczak et al. 2012; Woodhams et al. 1984). The samples with the reinforcement content around 40-50 % showed the best tensile properties with tensile strength around 50 MPa and Young's modulus around 8 GPa. The tensile properties seem unaffected by matrix pulp DP within the experimental errors. This phenomenon again was somehow unexpected, as far as longer polymer chains in the matrix should result in a stronger material. The reason is that higher

molecular weight is counterbalanced by lower concentration of dissolved cellulose in the matrix, see Table 1.

The values of tensile properties reported in this work are similar to those published previously on short-fiber reinforced all-cellulose composites (Nadhan et al. 2012; Abbot and Bismarck 2010; Ouajai et al. 2009; Duchemin et al. 2009; Yang et al. 2010). However, an adequate comparison with literature is difficult because of a significant variation in processing methods. Only two publications describe composite preparation via dispersion of reinforcing fibers in cellulose solution using NaOH-based solvent: cotton of DP around 600 was dissolved to make the matrix and either regenerated cellulose fibers (Nadhan et al. 2012) or ramie (Yang et al. 2010) were dispersed as reinforcement. The concentration of added fibers varied from 0 to 10 wt% in wet state. The tensile strength and Young's modulus of films were 50 - 80 MPa and 4-7 GPa (Nadhan et al. 2012) and 80 - 120 MPa and 4-6 GPa (Yang et al. 2010), respectively. While Nadhan et al. (2012) reported the increase in tensile properties with the increase of added fiber concentration (from 1 to 5% in wet state), Yang et al. (2010) demonstrated the decrease of tensile strength when the concentration of ramie exceeded 7% in wet state. They did not provide an explanation for the observed phenomenon.

Very few works report on all-cellulose composite density while it can explain the trends in mechanical properties. We plotted our data on Young's modulus as a function of density together with those published by Piltonen et al. (2016), Hildebrandt et al. (2017) and Kröling et al (2018), the results are shown in Figure 9. In the latter publication, paper from oriented fibers was impregnated with ionic liquid, 1-ethyl-3-methylimidazoium acetate. Young's moduli measured in fiber direction and in transversal direction are thus different (Figure 9). For isotropic composites all values fall on the same curve demonstrating modulus increase with the increase of density, which is expected for porous materials.

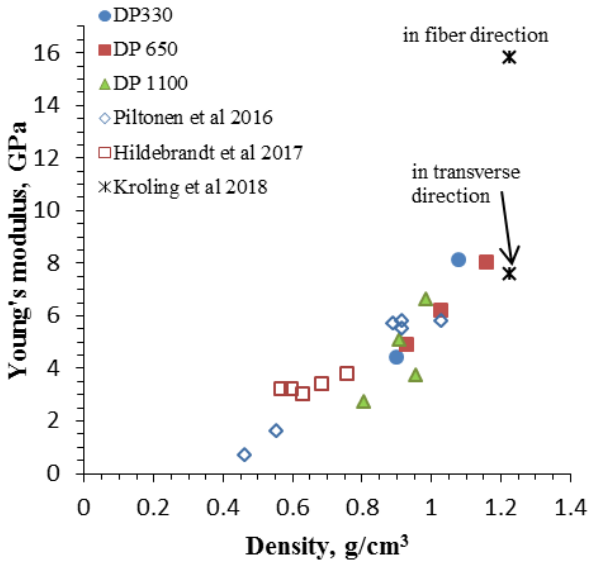

Fig. 9

All-cellulose composite Young's modulus as a function of density from this study compared with results shown by Piltonen et al. (2016), Hildebrandt et al. (2017) and Kröling et al (2018).

Ouajai et al. (2009) used NMMO monohydrate for making a matrix from 12% dissolved hemp and dispersing the same fibers at high concentration, 40% in wet state. The values of modulus were rather low, 1 – 2 GPa, and voids were noticed in the SEM images. Authors also reported an incomplete dissolution of hemp, which is similar to our case, but density (or porosity) was not provided. Finally, microcrystalline cellulose (MCC) was partly dissolved in LiCl/DMAc by varying the dissolution parameters and thus changing the proportion between dissolved and non-dissolved cellulose. Very different tensile properties were reported: from 0.7 – 1.5 GPa and 35 – 65 MPa (9% MCC, Abbot and Bismarck 2010) to 1 – 6 GPa and 20 – 100 MPa (5-20% MCC, Duchemin et al. 2009) and 12 – 15 GPa and 215 – 250 MPa (2 – 4 % MCC, Gindl and Keckes 2005) for Young's modulus and tensile strength, respectively. These results show that processing parameters play the key role even if making all-cellulose composites from the same starting materials and with similar approaches. Despite the increase in the crystallinity with the increase of MCC concentration (due to the increase of non-dissolved fraction of cellulose), Duchemin et al. 2009 reported the decrease in

tensile strength for several cases when MCC concentration exceeded 10 – 15% in wet state. The understanding of cellulose dissolution and its limits in a given solvent is crucial for the optimization of all-cellulose composite mechanical properties.

Conclusions

All-cellulose composites were prepared via dispersion of short softwood kraft fibers in the cellulose matrix based on solutions of dissolving pulp of various degrees of polymerization in 8 wt% NaOH-water. Mixtures were gelled, coagulated, washed from NaOH, compressed and dried. Cellulose dissolution in 8 wt% NaOH-water was shown to strongly decrease with the increase of pulp DP leading to a strong decrease in the actual concentration of dissolved cellulose in the matrix.

All-cellulose composited showed a decrease of tensile properties with the increase of total reinforcing fiber content, while the crystallinity of the composites was the same for the cases studied. High non-dissolved fiber content per insufficient amount of matter in the matrix was shown to create voids in the composite, as confirmed by SEM, decreasing the density from 1.16 to 0.81 g/cm^3 with the increase of reinforcing fibers. Density was shown to be the major contributor to mechanical properties of the composites. All-cellulose composites are complex materials and when analyzing their properties, several aspects must be considered. In addition to the classical parameters, such as reinforcing fiber concentration and properties, fiber-matrix adhesion and fiber distribution, solvent power and processing methods must be taken into account.

The tensile properties of all-cellulose composites obtained in this work compare well with those of wood-plastic composites, demonstrating the potential of all-cellulose composites in various applications. Processing is simple and various existing pulps can be used together with the cheap solvent. Low dissolving power of NaOH-water is not a disadvantage here provided an adequate selection of the DP of the dissolving pulps.

References

Abbot A, Bismarck A (2010) Self-reinforced cellulose nanocomposites. Cellulose 17:779-791. doi: 10.1007/s10570-010-9427-5

Alexander L, Klug HP (1948) Basic aspects of X-ray absorption in quantitative diffraction analysis of powder mixtures. Anal Chem 20:886-889

Ashiotis G, Deschildre A, Nawaz Z, Wright JP, Karkoulis D, Picca FE, Kieffer J (2015) The fast azimuthal integration Python library: pyFAI. Journal of applied crystallography 48:510-519

Budtova T, Navard P (2016) Cellulose in NaOH-water based solvents: a review. Cellulose 23:5-55

Brückner S (2000) Estimation of the background in powder diffraction patterns through a robust smoothing procedure. Journal of Applied Crystallography 33:977-979

Cao Y, Wu J, Zhang J, Li H, Zhang Y, He J (2009) Room temperature ionic liquids (RTILs): A new and versatile platform for cellulose processing and derivatization. Chemical Engineering Journal 147:13-21. doi: 10.1016/j.cej.2008.11.011

Capiati NJ, Porter RS (1975) The concept of one polymer composites modelled with high density polyethylene. Journal of materials science 10: 1671-1677. doi: 10.1007/BF00554928

Davidson GF (1934) The dissolution of chemically modified cotton cellulose in alkaline solutions. Part I: In solutions of NaOH, particularly at T°C below the normal. The Journal of the Textile Institute. 25:T174-T196

Dormanns JW, Schuermann J, Müssig J, Duchemin BJC, Staiger MP (2016) Solvent infusion processing of all-cellulose composite laminates using an aqueous NaOH/urea solvent system. Composites Part A 82:130-140. DOI: 1016/j.compositesa.2015.12.002

Duchemin BJC, Newman RH, Staiger MP (2009) Structure-property relationship of all-cellulose composites. Composites Science and Technology 69:1225-1230. doi: 10.1016/j.compscitech. 2009.02.027

532 Duchemin B, Corre DL, Leray N, Dufresne A, Staiger MP (2016) All-cellulose composites
533 based on microfibrillated cellulose and filter paper via NaOH-urea solvent system. Cellulose
534 23:593-609. Doi: 10.1007/s10570-015-0835-4
535 Egal M, Budtova T, Navard P (2007) Structure of aqueous solutions of microcrystalline
536 cellulose-sodium hydroxide below 0°C and the limit of cellulose dissolution. Biomacromolecules 8:
537 2282-2287. doi: 10.1021/bm0702399
538 Fink H-P, Weigel P, Purz HJ, Ganster J (2001) Structure formation of regenerated cellulose
539 materials from NMMO-solutions. Progress in Polymer Science 26:1473-1524. doi: 10.1016/S0079-
540 6700(01)00025-9.
541 Frost K, Kaminski D, Kirwan G, Lascaris E, Shanks R (2009) Crystallinity and structure of
542 starch using wide angle X-ray scattering. Carbohydr Polym 78:543-548
543 Gindl W, Keckes J (2005) All-cellulose nanocomposite. Polymer 46: 10221-10225. doi:
544 10.1016/j.polymer.2005.08.040
545 Gindl W, Schöberl T, Keckes J (2006) Structure and properties of a pulp fibre-reinforced
546 composite with regenerated cellulose matrix. Applied Physics A 83:19-22. doi: 10.1007/s00339-
547 005-3451-6
548 Haverhals LM, Sulpizio HM, Fayos ZA, Trulove MA, Reichert WM, Foley MP, De Long HC,
549 Trulove PC (2012) Process variables that control natural fiber welding: time, temperature and
550 amount of ionic liquid. Cellulose 19:13-22. Doi: 10.1007/s10570-011-9605-0
551 Hildebrandt N, Piltonen P, Valkama J, Illikainen M. 2017. Self-reinforcing composites from
552 commercial pulps via partial dissolution with NaOH/urea. Industrial Crops & Products. 109: 79-84.
553 doi: 10.1016/j.indcrop.2017.08.014
554 Huber T, Müssig J, Curnow O, Pang S, Bickerton S, Staiger MP (2012a) A critical review of
555 all-cellulose composites. Journal of Materials Science 47:1171-1186. Doi: 10.1007/s10853-011-
556 5774-3

Huber T, Pang S, Staiger MP (2012b) All-cellulose composite laminates. Composites: Part A 43:1738-1745. doi: 10.1016/j.compositesa.2012.04.017

Huber T, Bickerton S, Müssig J, Pang S, Staiger MP (2013) Flexural and impact properties of all-cellulose composite laminates. Composites Science and Technology 88:92-98. doi: 10.1016/j.compscitech.2013.08.040

Janson J (1970) Calculation of the polysaccharide composition of wood and pulp. Paperi ja puu 5: 323-329

Kamide K, Okajima K, Kowsaka K (1992) Dissolution of natural cellulose into aqueous alkali solution: role of super-molecular structure of cellulose. Polymer Journal 24-1:71-96. doi: 10.1295/polymj.24.71

Kröling H, Duchemin B, Dormanns J, Schabel S, Staiger MP (2018) Mechanical anisotropy of paper based all-cellulose composites. Composites Part A 113:150-157. DOI: 10.1016/j.compositesa.2018.07.005

Labidi K, Korhonen O, Zrida M, Hamzaoui A H, Budtova T (2019) All-cellulose composites from alfa and wood fibers. Industrial Crops & Products 127: 135-141

McCormick CL, Lichatowich DK (1979) Homogeneous solution reactions of cellulose, chitin and other polysaccharides to produce controlled-activity pesticide systems. Journal of Polymer Science: Polymer Letters Edition 17:479-484

Michud A, Hummel M, and Sixta H. 2015. Influence of molar mass distribution on the final properties of fibers regenerated from cellulose dissolved in ionic liquid by dry-jet wet spinning. Polymer. 75: 1-9. doi: 10.1016/j.polymer.2015.08.017

Nadhan AV, Rajulu AV, Li R, Jie C, Zhang L (2012) Properties of regenerated cellulose short fibers/cellulose green composite films. Journal of Polymers and the Environment. 20:454-458. doi: 10.1007/s10924-011-0398-x

Nishino T, Matsuda I, Hirao K (2004) All-cellulose Composite. Macromolecules 37:7683-7687. doi: 10.1021/ma049300h

Nishino T, Arimoto N (2007) All-cellulose composite prepared by selective dissolving of fiber surface. Biomacromolecules 8:2712-2716. DOI: 10.1021/bm0703416

Ouajai S, Shanks RA (2009) Preparation, structure and mechanical properties of all-hemp cellulose biocomposites 69:2119-2126 doi: 10.1016/j.compscitech.2009.05.005

Piltonen P, Hildebrandt N, Westerlind B, Valkama J, Tervahartiala T, Illikainen M. 2016. Green and efficient method for preparing all-cellulose composites with NaOH/urea solvent. Composites Science and Technology. 135: 153-158. Doi: 10.1016/j.compscitech.2016.09.022

Roy C, Budtova T, Navard P (2003) Rheological properties and gelation of aqueous cellulose-NaOH-solutions. Biomacromolecules 4: 259-264. doi: 10.1021/bm020100s

Savitzky A, Golay MJ (1964) Smoothing and differentiation of data by simplified least squares procedures. Anal Chem 36:1627-1639

Sobczak L, Lang RW, Haider A (2012) Polypropylene composites with natural fibers and wood – General mechanical property profiles. Composites Science and Technology 72:550-557

Sirviö JA, Visanko M, Hildebrandt NC (2017) Rapid preparation of all-cellulose composites by solvent welding based on the use of aqueous solvent. European Polymer Journal 97:292-298. doi: 10.1016/j.eurpolymj.2017.10.021

Soykeabkaew N, Arimoto N, Nishino T, Peijs T (2008) All-cellulose composites by surface selective dissolution of aligned lingo-cellulosic fibers. Composites Science and Technology 68:2201-2207. doi: 10.1016/j.compscitech.2008.03.023

Thygesen A, Oddershede J, Lilholt H, Thomsen AB, Ståhl K (2005) On the determination of crystallinity and cellulose content in plant fibres. Cellulose 12:563

Ward IM, Hine PJ (1997) Novel composites by hot compaction of fibers. Polymer Engineering and Science 37: 1809-1814. doi: 10.1002/pen.11830

Woodhams RT, Thomas G, Rodgers DK (1984) Wood fibers as reinforcing fillers for polyolefins. Polymer engineering and science 24: 1166-1171

Yang Q, Le a, Zhang L (2010) Reinforcement of ramie fibers on regenerated cellulose films. Composites Science and Technology 70:2319-1214. doi: 10.1016/j.compscitech.2010.09.012

Graphical abstract to

"All-cellulose composites via short-fiber dispersion approach using NaOH-water solvent"

By Oona Korhonen, Daisuke Sawada, Tatiana Budtova

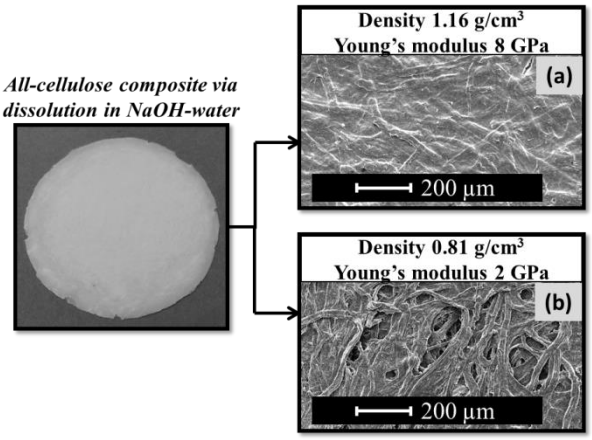

Morphology of all-cellulose composites : matrix is from low-DP dissolving pulp (a) and from high-DP 1110 pulp (b).